JOURNAL OF MATERIALS SCIENCE 15 (1980) 1755–1764

Etch features on synthetic diamond crystals oxidized in fused salts

N. J. PIPKIN
De Beers Diamond Research Laboratory, Johannesburg, South Africa

Scanning electron microscope studies have confirmed that synthetic diamonds, etched in fused salts, develop square pits with ⟨1 1 0⟩ oriented edges on the cube faces and positively oriented trigons on the octahedral facets. The pits on the {1 0 0} faces are bounded by {5 1 1} planes whilst those on the {1 1 1} facets are bounded by faces of the form {2 2 3}. Additional square pits on the {1 0 0} faces and which have ⟨1 0 0⟩ edges have been observed and are associated with the build-up of carbon dioxide and monoxide on the diamond surfaces. In some instances the ⟨1 1 0⟩ intersections of cube and octahedral faces become modified by the development of {2 1 1} facets. Other etch features are reported which correlate with the lines of intersection between the {1 1 1} slip planes and the {1 0 0}, {1 1 0} and {1 1 1} crystal faces. These are in the form of elongated etch pits.

1. Introduction

Numerous papers have been published on the subject of etch-pit formation on natural and synthetic diamond crystals, a few of which are cited here [1–5]. These studies have been concerned principally with the orientation of the pits formed on diamond surfaces as the result of attack by a number of different media. However, little attention has been paid to the nature of the facets bounding the pits formed on the various crystal faces until recently [6]. These latter workers indexed the pit faces on the {1 0 0} diamond facets as belonging to the form {13, 5 5} while pits on the octahedral crystal surfaces were bounded by {8 8 5} faces. The basis of their indexing technique was two-beam optical interferometry.

In a previous paper [7] it was shown that the scanning electron microscope (SEM) could be usefully employed for crystallographic measurements on small cyrstals. The work described here was carried out using the SEM as a means of measuring interfacial angles and thus of indexing the etch-pit faces. The results obtained are different from those reported by Watanabe *et al.* [6]. In addition, a number of new etching features which have been observed are described.

2. Experimental method

Oxidation experiments were performed in the temperature range 600 to 850° C, using fused sodium nitrate, potassium nitrate and sodium hydroxide. The experiments were carried out in alumina crucibles placed in a muffle furnace.

The diamonds were etched in the same way by all three fused salts over the whole temperature range examined, the only major difference being that the potassium nitrate reacted with the diamonds more vigorously than the other two salts.

3. Results and discussion

3.1. Etch-pit formation on {1 0 0} and {1 1 1} faces

The common form of etch pit observed on the cube faces was a square-based pyramid (Fig. 1), typical of those reported by previous workers [1, 3, 4]. The base of the pyramid lies within the plane of the {1 0 0} faces and the edges lie along ⟨1 1 0⟩ crystallographic directions.

Fig. 2a is a schematic drawing of one of these pits. Each pit is bounded by four $\{hkl\}$ planes, of which the plane oab is one example. The line of intersection of adjacent faces is a direction of the type $\langle uvw \rangle$. In Fig. 2a the $[uvw]$ direction represents the line of intersection of the $\{hkl\}$ faces oab and oac.

The direction $[u'v'w']$ is the line joining the pit apex, o, to the mid-point of the line ab. Since ab is a $[\bar{1}10]$ direction, it is not difficult to see

0022–2461/80/071755–10$03.00/0

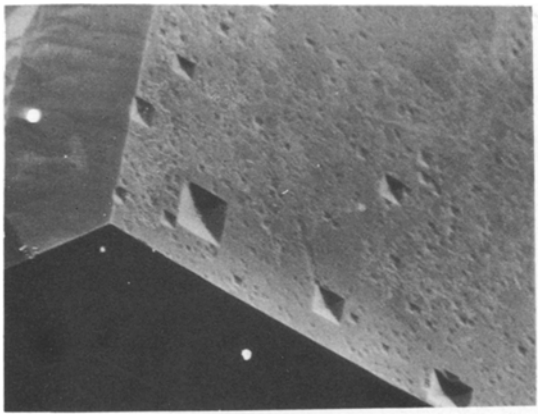

Figure 1 Etch pits with a ⟨110⟩ orientation on the diamond cube faces, × 2000.

that the $[u'v'w']$ direction is co-planer with the [001], [111] and [110] crystallographic directions and that this plane is the $(\bar{1}10)$ plane. Furthermore, the normal to the (hkl) face, oab, also lies in this same $(\bar{1}10)$ plane.

In a similar manner it can be seen that the directions [001], $[uvw]$, [101] and [100] are also co-planer, with the common plane having the indices (010). Fig. 3a and b show the relationship between these directions in both clinographic and stereographic representations, respectively.

The etch pits formed on the octahedral faces were trigons with a positive orientation (Fig. 4). Although many of these are whole triangular-based pyramids, a number of them are truncated.

Fig. 2b is a schematic drawing of a typical trigon on a $(1\bar{1}1)$ face. The directions $[u_1 v_1 w_1]$ and $[u_2 v_2 w_2]$ are the equivalents of the corresponding directions $[uvw]$ and $[u'v'w']$ shown in Fig. 2a. Again, since the line $a'c'$ is a [110] direction, it is clear that the directions $[1\bar{1}1]$, $[u_1 v_1 w_1]$ and [001] all lie in a (110) plane. Similarly, the $[1\bar{1}1]$, $[u_2 v_2 w_2]$, [101] and [111] directions and the normal to the $(h'k'l')$ plane $o'a'b'$ lie in a $(\bar{1}01)$ plane. These relationships can also be seen in Fig. 3a and b.

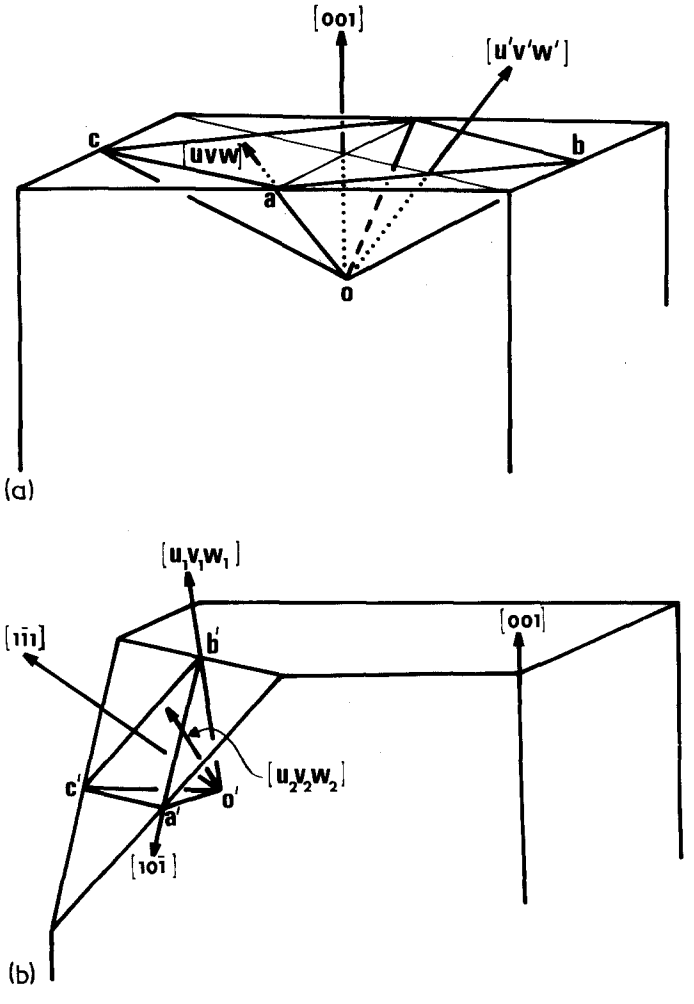

Figure 2 Schematic drawings of the etch pits formed on the cube faces (a), and on the octahedral faces (b).

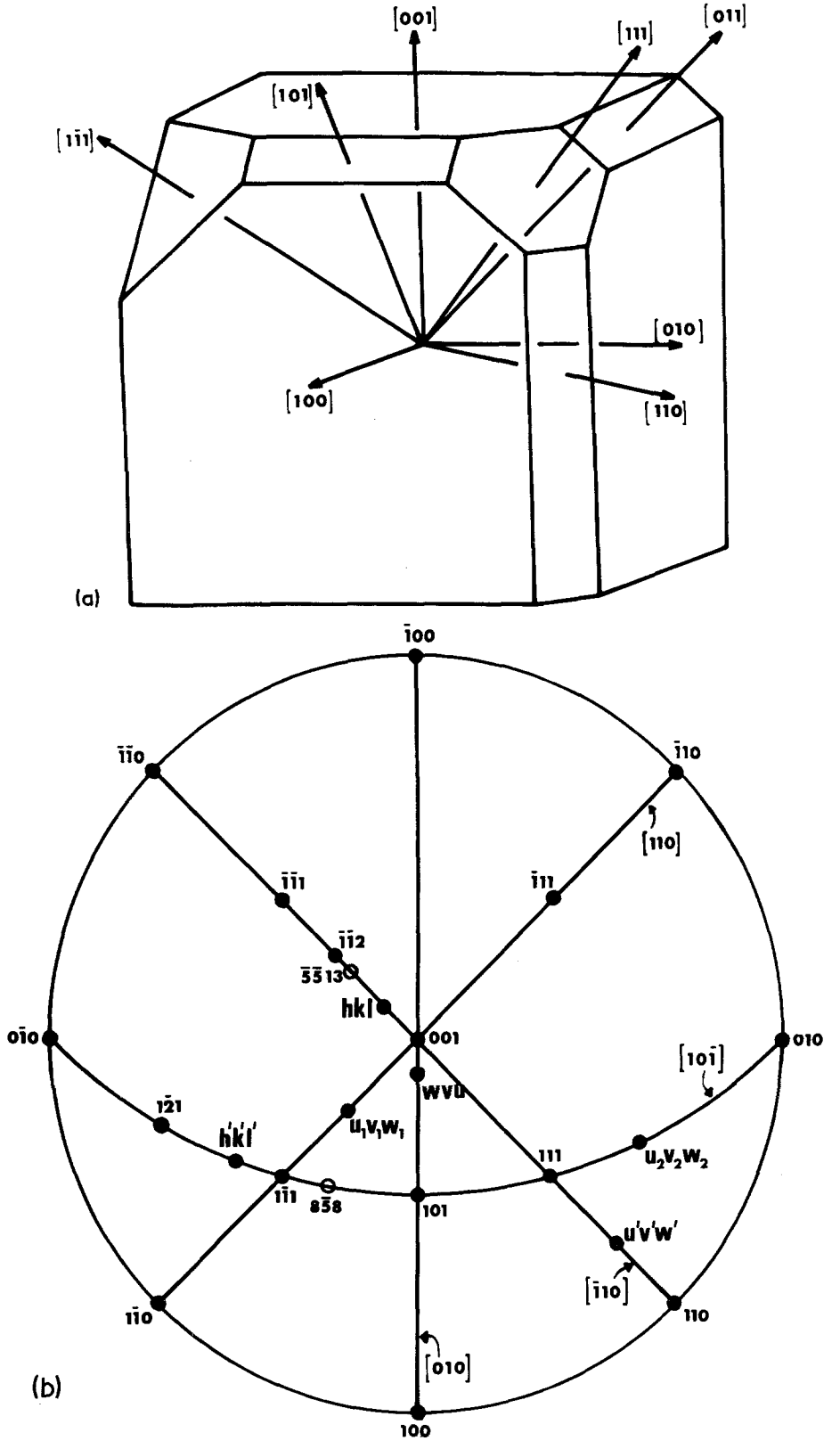

Figure 3 Clinographic (a) and stereographic (b) projections of a diamond crystal showing the relationship between the various crystal directions described in the text.

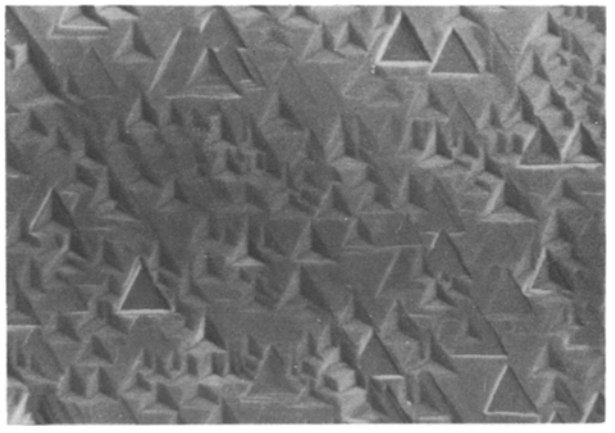

Figure 4 Trigons on the octahedral faces, X 1200.

Because of these simple relationships between the faces of the etch pits and the low index cube faces, measurement of the interfacial angles in the SEM is relatively straightforward using a modification of a technique described in a previous publication [7].

A typical crystal was mounted on a SEM stub with the (001) cube face lying parallel to the stub surface. In this way it was easy to orientate the crystal in the microscope with the [001] direction lying along the beam axis and with the goniometer tilt setting close to zero degrees. Fig. 5a shows the various directions in the (010) plane, in this initial orientation, relative to the beam direction, V. Tilting the crystal about the [010] direction brought the direction $[wvu]$ to coincide with the beam direction after a rotation, α, of 11.63° (Fig. 5b). (Note: the direction $[wvu]$ is used here to be consistent with the etch pit lying in a (100) plane.) The direction $[wvu]$, therefore, corresponds to a [105] direction, the calculated angle between an [001] and a [105] direction being 11.31°. (These values are considered to be the same within the accuracy of the technique.) Returning the crystal to its initial orientation and then tilting about the [110] direction permitted measurement of the angle between [001] and $[u_1\, v_1\, w_1]$ directions. The determined value of 30.09° is close to the angle between an (001) and a $(2\,\bar{2}\,5)$ direction which was calculated as 29.50°.

The crystal was remounted, so that the [111] direction lay parallel to the beam axis at zero tilt, and the etch pits on the (001) and $(1\,\bar{1}\,1)$ faces were examined. As shown in Fig. 5c and d, by rotating about a $[\bar{1}10]$ direction the angle between the [111] and $[u'v'w']$ directions can be determined. Because the $(\bar{1}\,\bar{1}\,2)$ direction is perpendicular to [111], and $[u'v'w']$ is a direction lying within the (hkl) plane, this angle must be the same as that between the $[\bar{1}\,\bar{1}\,2]$ and $[hk!]$ directions. The value measured was 20.20°, corresponding to the angle between $[\bar{1}\,\bar{1}\,2]$ and $[\bar{1}\,\bar{1}\,5]$ directions (the calculated value is 19.47°). It is concluded, therefore, that the faces (hkl) are of the form $\{1\,1\,5\}$. This is totally consistent with the direction $[uvw]$ being a ⟨105⟩ type direction. The faces oab and oac in Fig. 2a are $(\bar{1}\,\bar{1}\,5)$ and (115) planes, respectively, and the line of intersection of these two faces, $[uvw]$, is a [501] direction.

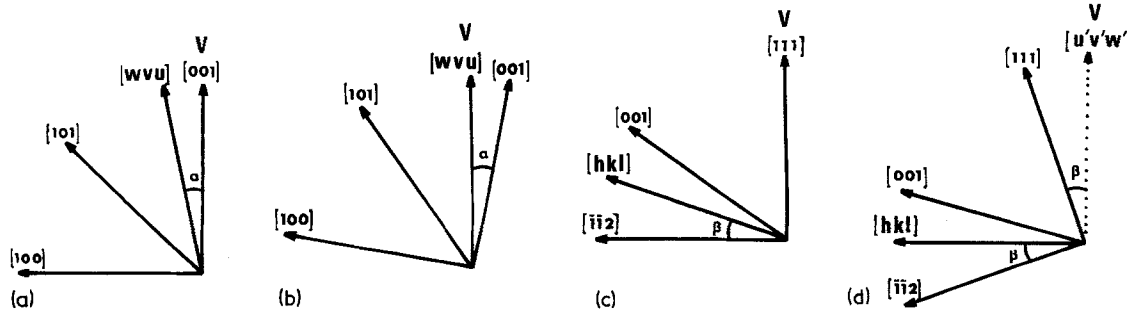

Figure 5 Measurement of the angles, in the SEM, between directions in the (010) plane (a, b) and in the $(\bar{1}10)$ plane (c, d).

Returning the crystal to the zero tilt position and then tilting again, this time about a $[10\bar{1}]$ direction, gave the angle between the $[u_2\, v_2\, w_2]$ and $[1\,\bar{1}\,1]$ directions as 7.59°. Since the $[1\,\bar{2}1]$ direction is normal to $[111]$, and $[u_2\, v_2\, w_2]$ is perpendicular to the $(h'k'l')$ plane normal $[h'k'l']$, this angle corresponds to that between the $(1\,\bar{2}1)$ and $(h'k'l')$ planes.

On this basis, therefore, the trigon faces are indexed as being of the form {223} since the calculated angle between $(1\,\bar{2}1)$ and $(2\,\bar{3}2)$ planes is 8.05°. The line of intersection of adjacent {223} faces is a ⟨225⟩ type direction. For example the line of intersection of the $(2\,\bar{3}2)$ and $(2\,\bar{2}3)$ faces is a $[52\bar{2}]$ direction.

It is concluded, therefore, that the normal etch pits, formed on synthetic diamonds by oxidation in sodium and potassium nitrates and in sodium hydroxide, in the temperature range 600 to 850° C, have a pyramid-shaped morphology; albeit often truncated in the case of pits formed on {111} facets. On the cube faces they are bounded by four planes of the form {115} and on the octahedral faces they are defined by the development of three {223} faces.

3.2. Anomalous etching on {100} faces

In previous publications [3, 4], it has been reported that, in addition to the square-based pits with the ⟨110⟩ orientation, further pits occasionally form which have their four sides lying along ⟨100⟩ directions. This has been ascribed to etching effects associated with the build-up of reaction products, since such pitting can be eliminated by agitating the fused salts during the oxidation experiments [4, 8].

In the present work, pits with a ⟨100⟩ orientation were occasionally found on the {100} faces. The particular characteristic of these pits is the rounded nature of the four edges of the square base (Fig. 6). Tilting, in the SEM, showed that the pit faces are also curved and, therefore, do not correspond with precise crystallographic planes. In general, a "hole" was observed at the pyramid apex, as is clearly seen in Fig. 6. It is suggested, therefore, that these particular pits are associated with surface defects or, perhaps, metal inclusions trapped during crystal growth. Large fissures in the diamond surfaces also showed etch characteristics strongly related to the ⟨100⟩ etch pits (Fig. 7).

All of these features are consistent with the view that the evolution of carbon dioxide monoxide is the cause of this etching phenomenon. Bubbles of gas will preferentially nucleate at surface defects and may adhere and grow throughout the etching experiments. It is reasonable to assume that the gas in the bubble will also further etch the diamond surface and will do so in a manner which stabilizes the formation of pits with a ⟨100⟩ orientation.

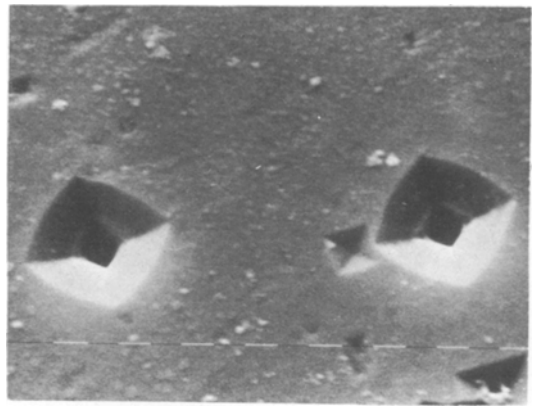

Figure 6 Pits with a ⟨100⟩ orientation formed on the cube faces, × 750.

Finally, it is often possible to find etch pits of the type shown in Fig. 8. These have a mixture of the characteristics of both etch pit types, leading to the formation of eight-sided pyramids. The four ⟨110⟩ edges are perfectly straight whereas the four ⟨100⟩ sides are curved. It is assumed that these occur when bubbles of gas nucleate in ⟨110⟩ pits which have been produced earlier in the oxidation process.

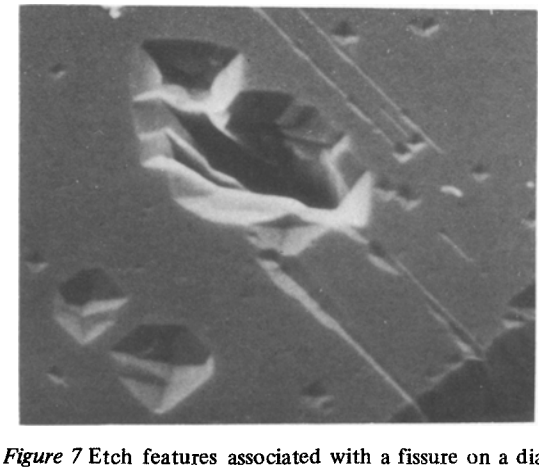

Figure 7 Etch features associated with a fissure on a diamond cube face, × 1000.

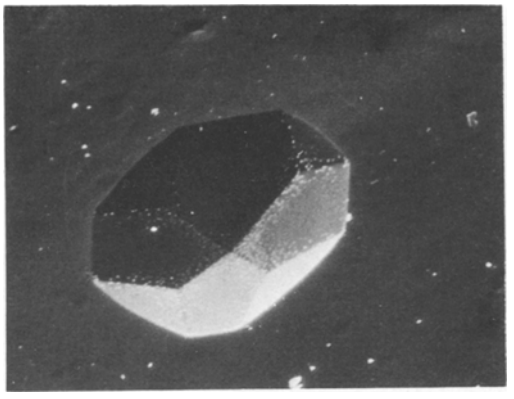

Figure 8 Etch feature showing the characteristics of both ⟨1 1 0⟩ and ⟨1 0 0⟩ pits, × 1800.

3.3. Compound etching effects

In a previous investigation [9], a further type of square-based pyramid etch pit was observed on the {1 0 0} faces of as-grown synthetic diamonds. The cause of these pits was back-etching by the metal solvents used in the synthesis process, and they are an indication that the temperature–pressure conditions moved from a diamond stable to a graphite stable region during the later stages of the growth cycle. The pits have a ⟨1 1 0⟩ orientation but, unlike those produced by oxidation in fused salts, they are bounded by {1 1 1} facets.

It was considered that these pits would act as nuclei for the generation of carbon monoxide and carbon dioxide so that the gas bubbles would build-up in these regions. In this way the pit morphology would be influenced by the gas rather than the fused salt and, therefore, the facets produced would be associated with gas etching. The results of experiments carried out with these crystals in molten sodium nitrate were surprising, although extremely interesting. For simplicity, in the following discussion, the {1 1 1} facetted pits will be referred to as the "primary pits".

Occasionally the orientation of the primary pits was found to change in the manner originally expected; that is from a ⟨1 1 0⟩ orientation to a ⟨1 0 0⟩ one (Fig. 9a). In general, however, the oxidation process produced the pit morphologies

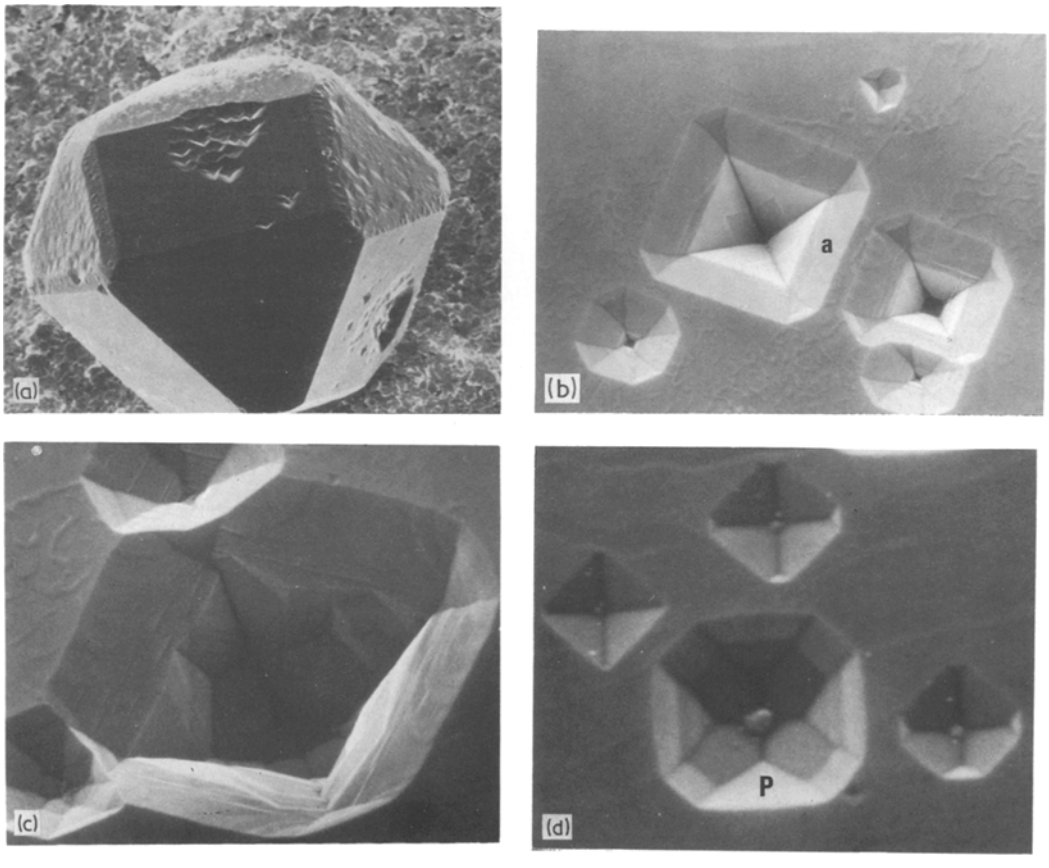

Figure 9 Oxidation characteristics of crystal which have undergone back-etching during growth. (a) × 50; (b) × 180; (c) × 400; (d) × 600.

shown in Fig. 9b and c. The principal effect of etching was the chamfering of the ⟨1 1 0⟩ edges of the primary pit by the development of a set of $\{hkl\}$ faces (e.g. at *a* in Fig. 9b). The indices of these facets were determined by tilting the crystal in the manner described earlier in Section 3.1 and were shown conclusively to be of the form {2 1 1} and not {5 1 1}. However, as can be seen in Fig. 9d, etch pits with {5 1 1} facets are generated on the smooth areas of the cube faces.

In addition to the {2 1 1} chamfering of the ⟨1 1 0⟩ edges of the primary pits, the line of intersection of adjacent {2 1 1} faces is further modified by the development of another set of planes which intersect the cube face along ⟨1 0 0⟩ directions. Thus is is possible to interpret the oxidation effects in this case as the superimposition of square pits with ⟨1 1 0⟩ and ⟨1 0 0⟩ orientations, respectively, in a manner similar to that shown in Fig. 8. The relative degree of development of the ⟨1 0 0⟩ pit orientation, compared with that of the ⟨1 1 0⟩ pit component, appeared to increase as the primary pit size decreased.

An interesting feature in Fig. 9d is the presence of a pit, P, in which the two etch pit morphologies cited here and those described in Section 3.1. are combined.

The reason for this change in the nature of the pit faces which are formed during the oxidation process is not clear. However, it seems that it is not simply a consequence of the build-up of reaction products, since all of the ⟨1 1 0⟩ edges of the cubo-octahedral crystal shown in Fig. 9a are also modified by {2 1 1} facets formed during the oxidation process. It is extremely unlikely that a gaseous atmosphere could be produced in the region of these crystal edges. Further, the pit shown in Fig. 9c appears to have developed {5 1 1} type faces at its apex. It is concluded, therefore, that the {2 1 1} facetting is a result of etch characteristics peculiar to the oxidation of sharp crystal edges.

Whether the {2 1 1} or the {5 1 1} faces are the more stable set of facets in these oxidizing environments is also uncertain at present. It may be that there is a geometric factor, associated with sharp edges, that overrides the chemical behaviour.

Finally, there are two other interesting aspects associated with these particular experiments. First, etch features are generated on the {1 1 1} faces of the primary pits. Sometimes these are pyramid shaped trigons (Fig. 9c), while in other cases they take the form of impressions based on flat trigons (Fig. 9b). Second, boat-shaped pits lying along ⟨1 1 0⟩ directions are often observed on the {2 1 1} faces (Fig. 9b and c).

3.4. Etching along slip planes

The common slip planes in diamond are the {1 1 1} planes which intersect the {1 0 0}, {1 1 0} and {1 1 1} crystal faces along ⟨1 1 0⟩ directions. In the case of the {1 1 0} facets the lines of intersection of four of the {1 1 1} faces lie along ⟨1 1 2⟩ directions, whereas the four remaining {1 1 1} planes cut the {1 1 0} faces along ⟨1 1 0⟩ directions.

Over the whole temperature range investigated, etch features which could clearly be associated with the intersection of the slip planes with the {1 0 0} facets were observed on the diamond cube faces. Typical examples are shown in Fig. 10a and b. In some cases, rows of overlapping etch pits lie along specific ⟨1 1 0⟩ type directions, whereas other etch features are characterized by the formation of pits which are markedly elongated in one of the two ⟨1 1 0⟩ directions. In Fig. 10b both possible orientations of these elongated pits can be seen.

Despite this modification to the etch pit shape, no change in the nature of the faces which define the morphology of the pits occurs.

Similar effects were observed on the octahedral faces (Fig. 10c) where etch traces, associated with the three ⟨1 1 0⟩ lines of intersection of the {1 1 1} slip planes, can be produced. Since the electron beam direction in Fig. 10c does not lie along the (1 1 1) plane normal, the measured angles between adjacent etch traces are not 60°. However, in the correct orientation, these angles were measured in the SEM and the expected value of 60° was confirmed.

Such features on the octahedral faces were observed only at the lower end of the temperature range examined, up to about 700° C. Above this temperature the particularly rapid formation of large trigons swamped this lighter etching feature.

The {1 1 0} faces were the most resistant to oxidation of the three low index families of planes. However, as shown in Fig. 10d, examples of etching on the dodecahedral faces are observed and these correlate with the intersection of {1 1 1} slip planes with the {1 1 0} faces. The angles between the long axes of these elongated pits and the [1 0 0] intersection of the (0 1 1) face and the adjacent (0 0 1) face is close to 35.16°. Conversely, the angle between these pit axes and the $[10\bar{1}]$

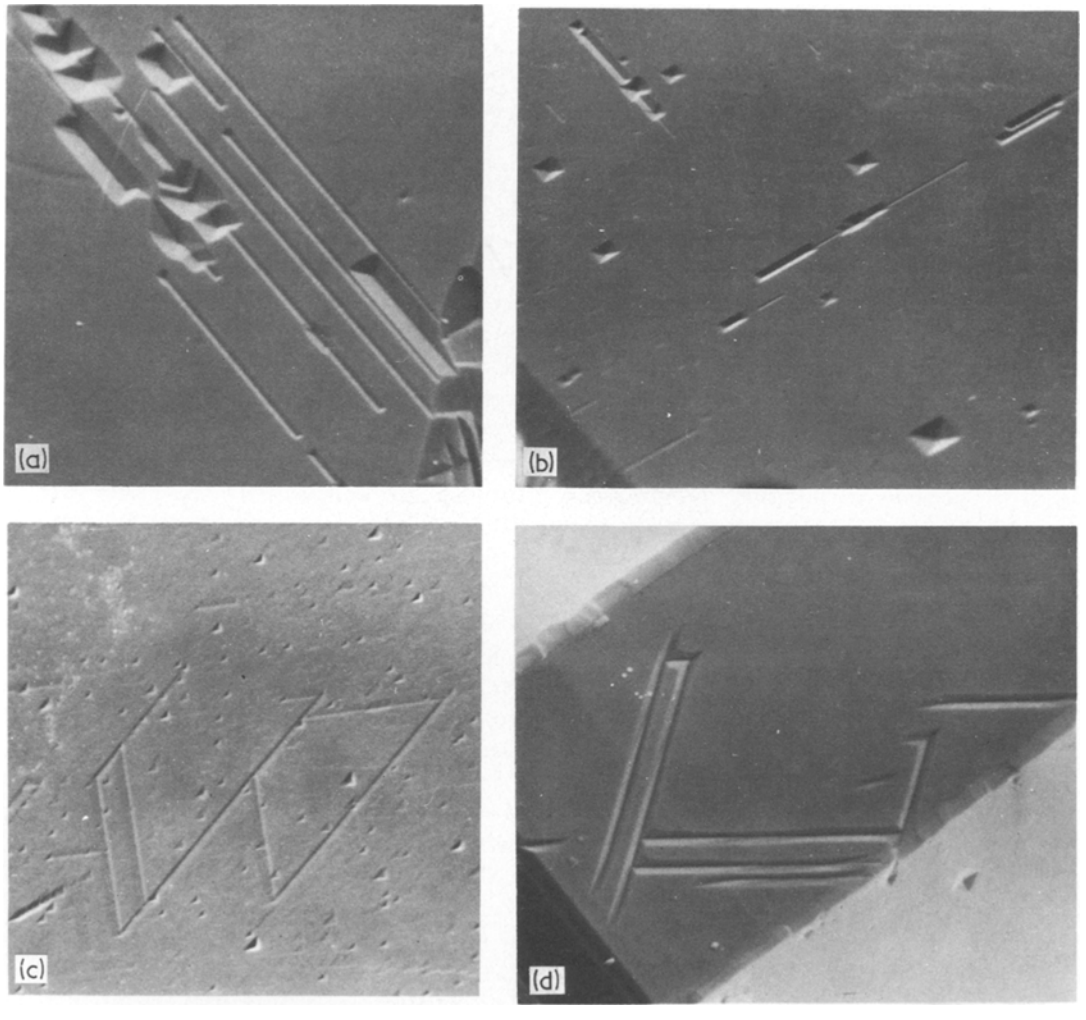

Figure 10 Linear etch pits formed on cube faces (a) × 2000; (b) × 750, on octrahedral faces (c) × 1800, and on dodecahedral faces (d) × 2000.

intersection of the (011) and (111) faces is 54.73°. In addition, the angle between the long axes of adjacent pits is close to the value of 74.54° expected for sets of ⟨112⟩ directions.

The origin of these etch features is not certain, but it does not seem unreasonable to suggest that they are associated with dislocations whose cores lie along ⟨110⟩ directions in the {111} slip planes. The driving force for preferential oxidation of this type could be either the dislocation strain field itself or the chemical effects associated with impurity atoms which have condensed along the dislocation cores. Alternatively, it could be a function of layered growth which was cited by Pandya and Tolansky [1] as a cause of etch lines on the (111) faces of natural diamonds. To support this latter hypothesis, some interesting micrographs are shown in Fig. 11a and b. In this case the etch lines on the (100) face correlate directly with similar etch features on the (110) face.

4. Further discussion

The results presented here contradict those reported by Watanabe *et al.* In their case, although the angle between the faces of the trigons and the {111} facets on which they form is, to all intents and purposes, the same, they index the faces as being of the form {885}, whereas in the present work they are indexed as {223} facets. As can be seen in Fig. 12, the poles of these faces lie on diametrically opposite sides of the (111) pole. The significance of this is that, whereas in the present

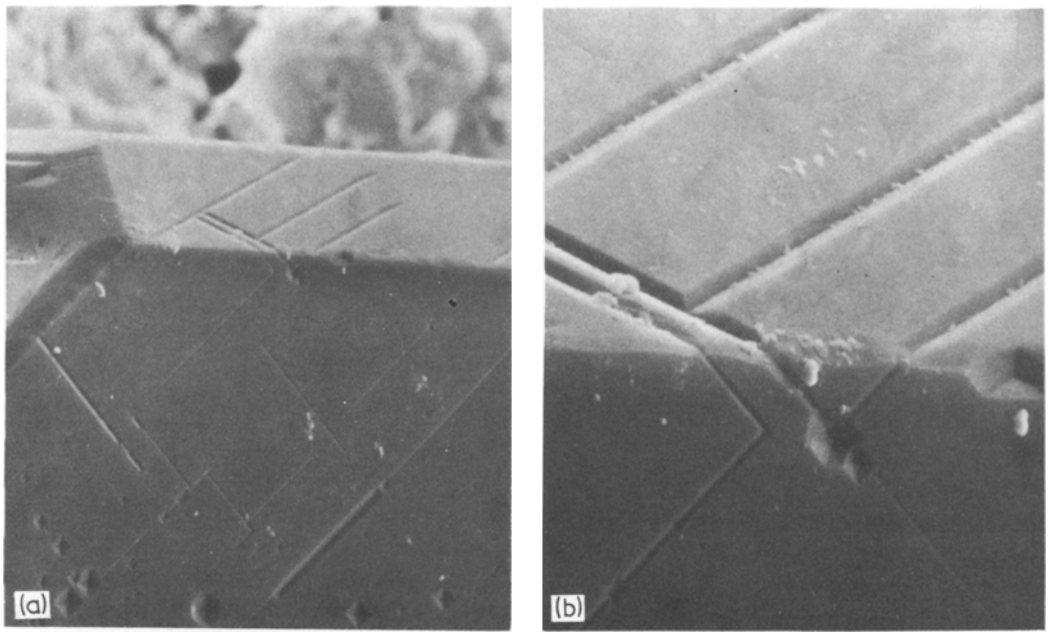

Figure 11 Correlation between linear etch features on the cube and dodecahedral faces (a) X 1200; (b) X 4000.

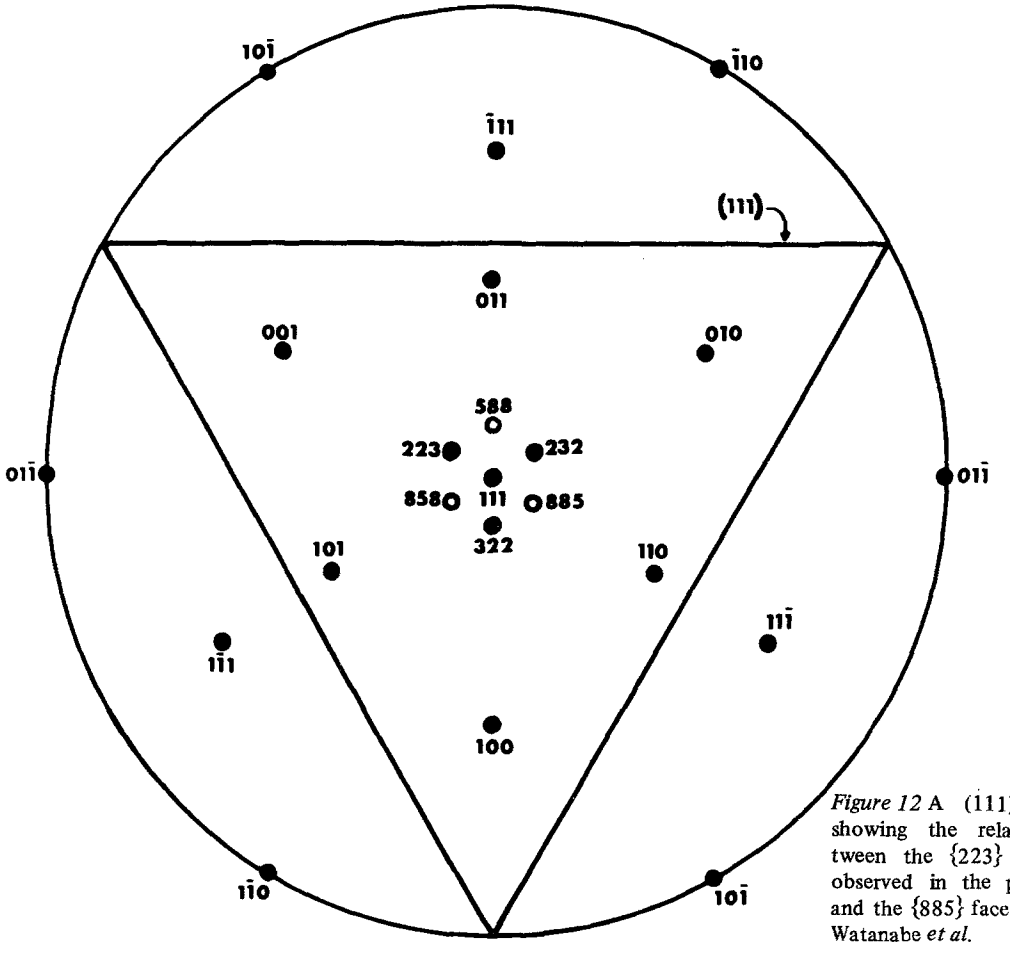

Figure 12 A (111) stereogram showing the relationship between the {223} trigon faces observed in the present work and the {885} faces reported by Watanabe *et al.*

case the trigons formed have a positive orientation, those observed by Watanabe *et al.* [6] must necessarily have a negative orientation.

For pits formed on the cube faces of the diamonds, the indices of the faces are entirely different in the two studies. Without additional data it is not possible to offer an explanation for this apparent anomaly.

One obvious difference between the two studies is the temperature range used in the fused potassium nitrate experiments. Watanabe *et al.* [6] investigated the range 475 to 525° C, whereas in the present work higher temperatures between 600 and 800° C were used. Omar *et al.* [10] reported that, on {1 1 1} crystal faces, etching proceeded in three stages. Stage one occurred between 500 and 550° C, stage two between 550 and 625° C and stage three at higher temperatures. This may possibly be the case on the cube faces also, thereby producing different etch pit morphologies at different temperatures.

5. Conclusions

The etch pits formed on the cube faces of synthetic diamonds, oxidized in fused potassium nitrate or sodium nitrate at 600 to 800° C, have a ⟨1 1 0⟩ orientation and are bounded by {5 1 1} facets, whereas those produced on the octahedral faces are positively oriented trigons bounded by facets of the form {2 2 3}. However, where sharp ⟨1 1 0⟩ crystal edges are present, these become modified by the development of {2 1 1} planes and not by either of the two faces mentioned above.

As reported in previous works, square pits with a {1 0 0} orientation are also sometimes observed on the {1 0 0} faces and some of the crystallographic features associated with them appear to be consistent with the suggestion that they are a result of the build-up of reaction products at specific points on the diamond surfaces. Other etch features are observed, on the {1 0 0}, {1 1 0} and {1 1 1} crystal faces, which can be correlated with the lines of intersection of the {1 1 1} slip planes with these faces. The origin of these features is uncertain but may be associated with dislocations lying within the body of the diamonds or with a layered process as the crystal growth mechanism.

References

1. N. S. PANDYA and S. TOLANSKY, *Proc. Roy. Soc. A.* **225** (1954) 40.
2. A. R. PATEL and S. TOLANSKY, *ibid.* **243** (1957) 41.
3. T. EVANS and D. H. SAUTER, *Phil. Mag.* **6** (1961) 429.
4. S. TOLANSKY, R. F. MILLER and J. PUNGLIA, *ibid.* **26** (1972) 1275.
5. A. R. PATEL and T. C. PATEL, *J. Appl. Cryst.* **4** (1971) 207.
6. J. WATANABE, F. YOSHINO and T. HASEGAWA, *J. Gem. Soc. Japan* **3** (1978) 9.
7. N. J. PIPKIN and G. J. DAVIES, *Proc. Elect. Soc. SA* **8** (1978) 127.
8. T. EVANS and C. PHAAL, "The kinetics of the diamond-oxygen reaction". Proceedings of the Fifth Biennial Conference on Carbon, Pennsylvania State University.
9. N. J. PIPKIN and G. J. DAVIES, unpublished work.
10. M. OMAR, N. S. PANDYA and S. TOLANSKY, *Proc. Roy. Soc. A.* **225** (1954) 33.

Received 9 October and accepted 13 November 1979.